Title	Welding Deformation of Plates with Longitudinal Curvature(Mechanics, Strength & Structure Design)
Author(s)	Luo, Yu; Ishiyama, Morinobu; Murakawa, Hidekazu
Citation	Transactions of JWRI. 1999, 28(2), p. 57-65
Version Type	VoR
URL	https://doi.org/10.18910/9411
rights	
Note	

Welding Deformation of Plates with Longitudinal Curvature†

Yu LUO*, Morinobu ISHIYAMA and Hidekazu MURAKAWA*****

Abstract

Welding deformation of plates with longitudinal curvature is analyzed by thermal-elastic-plastic FEM. The phenomena are clarified from the aspect of the inherent strain. Conceptually, both welding distortion and welding residual stress are produced by the inherent strain. The integration of the inherent strain gives the inherent deformations and the tendon force. The effect of the longitudinal curvature is closely examined. Further, a method to predict the welding deformation by elastic FEM using the inherent deformations and the tendon force is proposed and its validity is demonstrated through numerical examples.

KEY WORDS: (Welding deformation) (Curved plate) (Inherent strain) (Angular distortion) (Transverse shrinkage) (Longitudinal shrinkage) (Elastic analysis)

1. Introduction

Welding is a key technology for building metal structures such as ships and bridges. However, welding generally produces welding distortions due to shrinkage during the thermal cycle. To build metal structures with required precision, the welding distortion in all stage of assembly must be taken into account. The welding distortion can be separated into the angular distortion, the transverse shrinkage and the longitudinal shrinkage. The levels of the welding distortion depend mostly the heat input and the thickness of the plate and they can be determined either by experiment or by thermal-elastic-plastic analyses. It is relatively easy to predict the welding distortion in a simple specimen in a laboratory. But the prediction of the welding distortion in large scale practical structures cannot be achieved by simple experiment or by thermal-elastic-plastic FEM.

On the other hand, the shrinkage at the welding joint is mostly determined by the heat input and the plate thickness and its distribution along the weld line is almost uniform. Thus, if the shrinkage at the weld joint (inherent deformation) is known then the welding deformation of a large structure can be predicted by elastic FEM analysis[1), 2), 3)]. In this report, the inherent deformation in both flat and curved plates are defined using the thermal-elastic-plastic FEM and the effect of longitudinal curvature is closely examined. Further, a method to predict the welding deformation by elastic FEM using the inherent deformations and the tendon force is proposed and its validity is demonstrated through numerical examples.

2. T-E-P Analysis of Bead Welding on Plate

2.1 Model for analysis

The bead welding on a rectangular plate with length: 1000 mm, width: 1000 mm and thickness: 12 mm shown in **Fig. 1** is analyzed. The material of the plate is mild steel with the temperature dependent thermal and mechanical properties shown in **Figs. 2** and **3**. Six cases with different heat input shown in **Table 1** are

Table 1 Welding condition.

	Case1	Case2	Case3	Case4	Case5	Case6
Speed (mm/Sec)	7.0	7.0	7.0	7.0	7.0	7.0
Thermal efficiency	0.75	0.75	0.75	0.75	0.75	0.75
Q (J/mm)	432.0	864.0	1296.0	1728.0	2160.0	2592.0
Q/h^2 (KJ/CM^3)	3.0	6.0	9.0	12.0	15.0	18.0

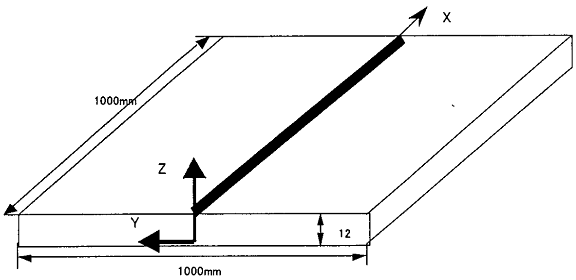

Fig.1 Analysis model.

† Received on November 29, 1999
* IEM
** Ishikawajima Harima Heavy Industries
*** Associate Professor

Transactions of JWRI is published by Joining and Welding Research Institute of Osaka University, Ibaraki, Osaka 567-0047, Japan.

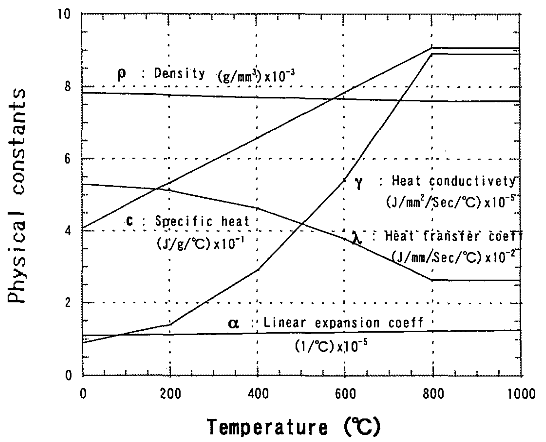

Fig.2 Temperature dependent thermal and physical constants.

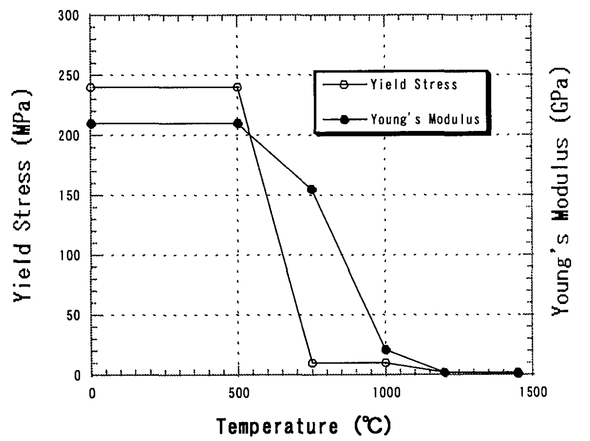

Fig.3 Temperature dependent mechanical properties.

analyzed as three dimensional thermal-elastic-plastic problems. The computed results are closely examined from the aspect of inherent deformation.

The problem is solved using ABAQUS employing the “DC3D8” element and the “C3D8I” element for thermal and stress analyses, respectively. Considering the symmetry, half of the plate is analyzed. The half plate is uniformly divided into 50 and 4 elements in the welding and the thickness directions. Non-uniform meshes with smaller elements near the welding line are employed in the width direction. The size of the smallest element near the welding line is 7.8 mm.

2.2 Computed results and discussions

2.2.1 Inherent deformations and tendon force

Conceptually, both welding deformation and welding residual stress are produced by the inherent strain. The concept of inherent strain can be generalized as the inherent transverse shrinkage, the inherent angular distortion and the tendon force, which arise from the integration of the inherent strain existing in the welding joint. When the components of the inherent strain are denoted by $(\varepsilon^*_x, \varepsilon^*_y)$, the tendon force: F, the inherent transverse shrinkage : δ_y and the inherent angular distortion : θ can be defined by the following equations.

Tendon force

$$F = \int E\varepsilon_x^* dydz \qquad (1)$$

Inherent transverse shrinkage

$$\delta_y = \frac{1}{h}\int \varepsilon_y^* dydz \qquad (2)$$

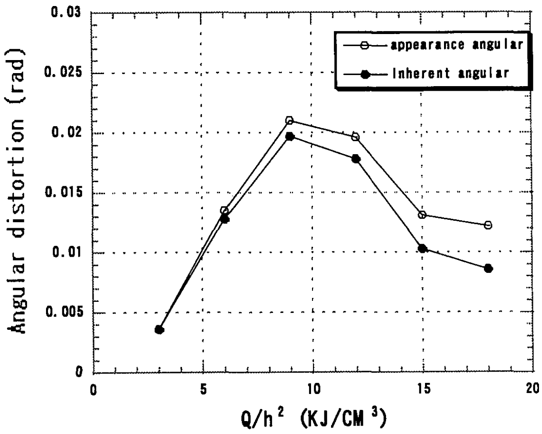

Fig.4 Effect of heat input on angular distortion.

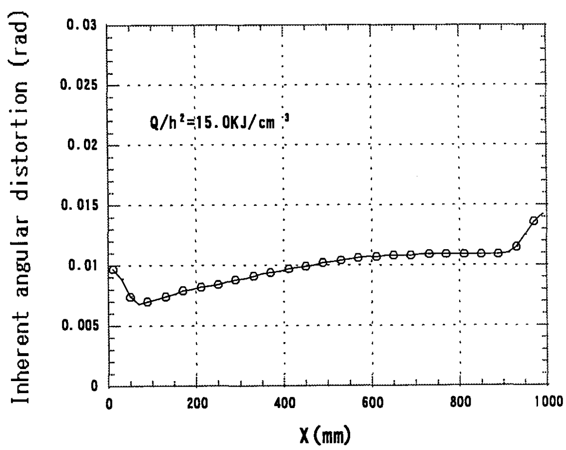

Fig.5 Distribution of inherent angular distortion along welding line.

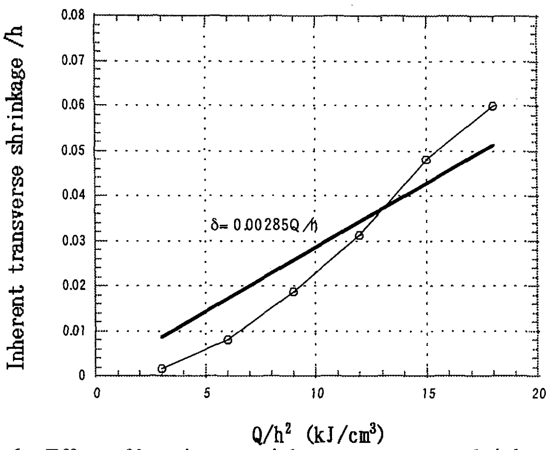

Fig.6 Effect of heat input on inherent transverse shrinkage.

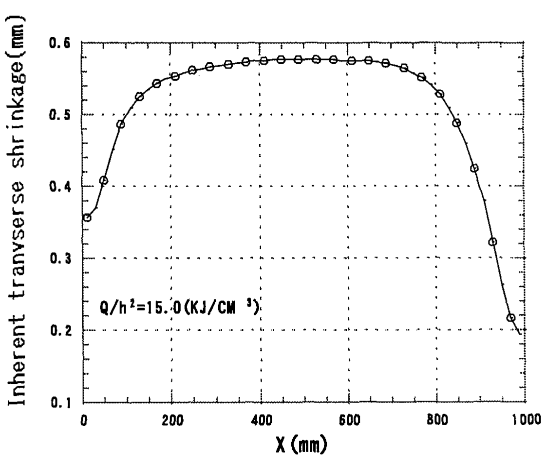

Fig.7 Distribution of inherent transverse Shrinkage along welding line.

Inherent angular distortion

$$\theta = \frac{1}{I}\int \varepsilon_y^*(z - h/2)dydz \qquad (3)$$

where,

$$I = \int (z - h/2)^2 dz$$

E: Young's modulus
h: Thickness of plate
ε^*_x : Inherent strain in welding direction
ε^*_y : Inherent strain in transverse direction

In case of the thermal-elastic-plastic analysis of the bead on plate problem, the plastic strain produced by the thermal cycle becomes the inherent strain. Thus the integrations of the plastic strain according to Eqs. (1), (2) and (3) gives the tendon force, the inherent transverse shrinkage and the inherent angular distortion. Once the inherent deformations and the tendon force are known for the given welding joint, the welding deformation can be computed by elastic analysis in stead of 3-dimensional thermal-elastic-plastic analysis. Thus the computed results of the serial thermal-elastic-plastic analysis are closely examined from the aspect of the inherent deformation in the next section.

2.2.2 Computed results

Figure 4 shows the comparison between the apparent angular distortion directly obtained by the thermal-elastic-analysis and the inherent angular distortion computed by Eq. (3). The figure shows the relation between the heat input parameter Q/h^2 and the angular distortions at the middle section of the plate. Q is the heat input per unit length. In general, the apparent angular distortion is larger than the inherent angular distortion. When the heat input is small, the difference between the apparent and inherent angular distortion is negligibly small. With an increase of the heat input, the difference becomes larger. This phenomenon can be explained as the influence of the tendon force. The tendon force increases with an increase of heat input and its influence on the apparent angular distortion becomes larger.

On the other hand, **Fig. 5** shows the distribution of the inherent angular distortion along the welding direction for the case with Q/h^2=15.0 kJ/cm^3 as an example. Though a slight increase at both the starting and the finishing ends is observed, the angular distortion increases from the starting end to the finishing end and it reaches the constant value after the welding length becomes greater than 600 mm in this case.

Similarly, the relation between the inherent transverse shrinkage at the middle section and the heat input parameter is shown in **Fig. 6**. In Fig. 6, the equation proposed by Satoh is plotted for comparison. Satoh suggested that the transverse shrinkage is roughly same as the thermal expansion causes by the welding heat input Q and proposed the following equation.

$$\delta = 2.85\times10^{-3}\ Q/h \qquad (4)$$

Also, the distribution of the inherent transverse shrinkage along the welding direction is shown in **Fig. 7**. The inherent transverse shrinkage is uniformly distributed except near the ends. Its value at both the starting and the finishing ends are considerably small and the length showing such local distribution is larger compared to the case of inherent angular distortion.

Further, the relation between the tendon force at the middle section and the heat input parameter is shown in **Fig. 8**. Generally, the tendon force increases with the

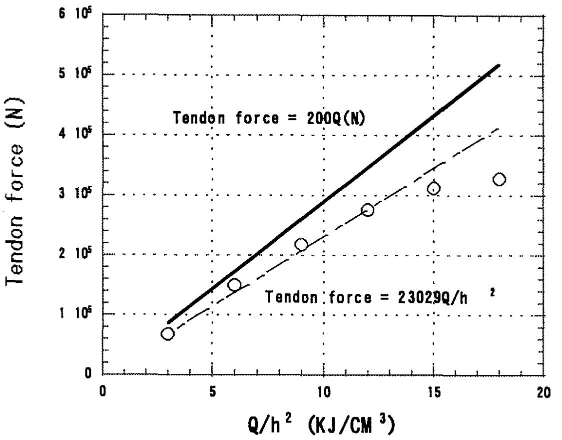

Fig.8 Effect of heat input on Tendon Force.

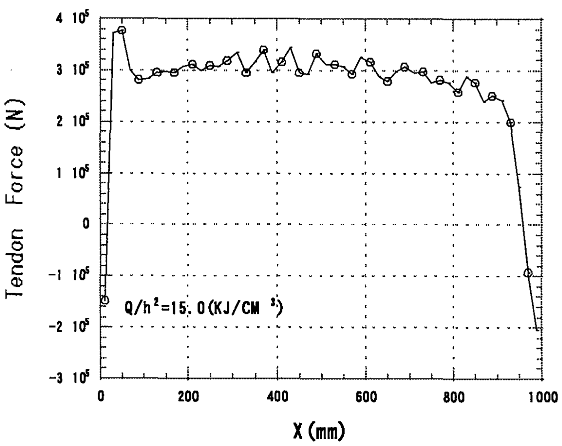

Fig.9 Distribution of Tendon force along welding line.

heat input but the rate of increase becomes small when the heat input increases. The chain line in Fig. 8 is the linear regression line for the computed results and the solid line represents the tendon force computed according to the following equation.

$$\text{Tendon force: } F=200Q(N) \qquad (5)$$

The distribution of the tendon force along the welding direction is shown in **Fig. 9**. The tendon force distributes uniformly except at the very ends of the plate. As seen from Figs. 5, 7 and 9, the distribution of the inherent deformations and the tendon force is almost uniform along the welding line except at the ends. This suggests that the distribution of the inherent deformations and the tendon force can be assumed constant along the welding line without serious loss of accuracy in prediction of welding deformation.

3. T-E-P Analysis of Bead Welding on Plate with Longitudinal Curvature

In the preceding section, the welding deformation of a flat plate under bead welding was studied. In this section, the welding deformation of a plate with longitudinal curvature is analyzed as a thermal-elastic-plastic problem using 3-dimensional FEM and the effect of the longitudinal curvature on the inherent deformations and the tendon force is examined.

3.1 Model for analysis

The dimensions of the plate are the same as those of the flat plate. Only the shape of the plate becomes cylindrical with a longitudinal curvature. Thus, the z-coordinate of the cylindrical plate Z is given by the following equation.

$$Z = Z_0 \pm \left(\sqrt{R^2-(x-L/2)^2} - \sqrt{R^2-(L/2)^2}\right) \qquad (6)$$

Where, Z_0: z-coordinate of flat plate
x: x-coordinate of flat plate
L: length of plate
R: radius of curvature

As for the welding condition, Case 3 (Q/h^2=9.0 kJ/cm^3) is selected as an example. To clarify the effect of the curvature 1/R, six cases with different values of the curvature, namely 1/R=0.001 mm, 0.0005 mm and 0.000333 mm (welding on the concave side of the plate) and 1/R=-0.001 mm, -0.0005 mm and -0.000333 mm (welding on the convex side of the plate) are analyzed. The inherent deformations and the tendon force are computed according to Eqs. (1), (2) and (3). Strictly speaking, the inherent strain defined on the local coordinate along the curved plate must be used in these equations. In the present computation, the coordinate transformation of the strain components is neglected. The order of the error due to this approximation is about 6% at the end of the plate in case of the plate with the largest curvature (1/R=0.001).

3.2 Computed results and discussions

The effect of longitudinal curvature on the inherent angular distortion is shown in **Fig. 10**. As shown in the figure, the inherent angular distortion decreases with the curvature. This tendency is more significant in cases where welding is on the convex side compared to the concave side. **Figure 11** shows the distribution of the inherent angular distortion along the welding line. Though the values themselves are quite different, their

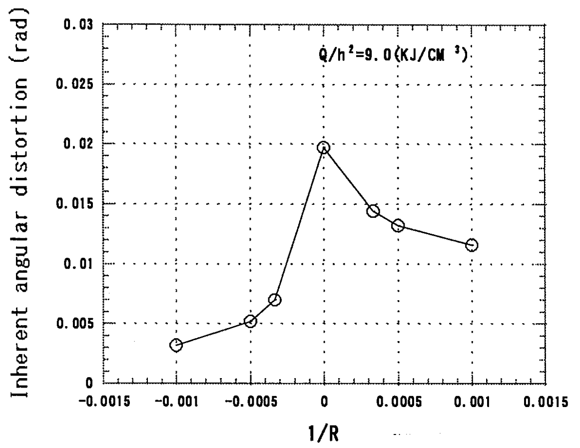

Fig.10 Effect of curvature on inherent angular distortion.

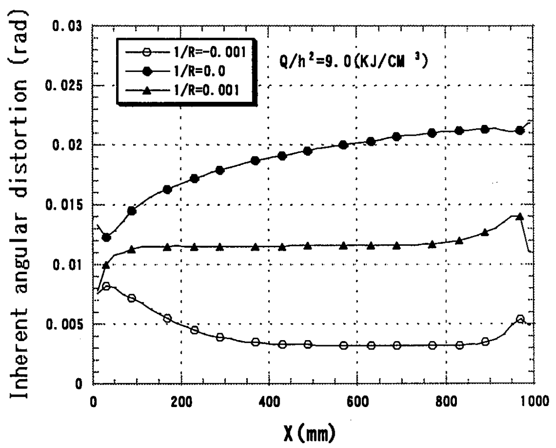

Fig.11 Comparison between distribution of inherent angular distortion in plates with different curvature.

distribution is fairly uniform except at the ends and regardless of the magnitude of the curvature. Comparing the welding on the concave and the convex sides, the welding on the concave side is closer to the flat plate.

Similarly, computed results for the transverse shrinkage are shown in **Figs. 12** and **13**. As observed clearly from these figures, the effect of longitudinal curvature on the inherent transverse shrinkage is quite small.

Figure 14 shows the influence of curvature on the tendon force. In case of welding on the concave side, the tendon force decreases with curvature. While in the case of the convex side, the tendon force increases with curvature when the curvature is small, and it decreases when the curvature exceeds –0.0005 (1/mm). **Figure 15** shows the influence of the direction of the curvature on the distribution of the tendon force along the welding direction. Significant differences are observed in both the magnitude and the distribution.

4. Elastic Computation Using Inherent Strain

The inherent deformations and the tendon force in bead welding on the flat plate and the curved plate with longitudinal curvature are clarified in Section 2 and 3. Once the inherent deformations and the tendon force are known, it becomes possible to predict the welding deformation of complex structures by elastic plate analysis instead of 3-dimensional thermal-elastic-plastic analysis. Thus, the detailed procedure for the elastic analysis is discussed in this section. Depending on the FEM code, the procedure may be different due to the available options. In this report, ABAQUS is selected

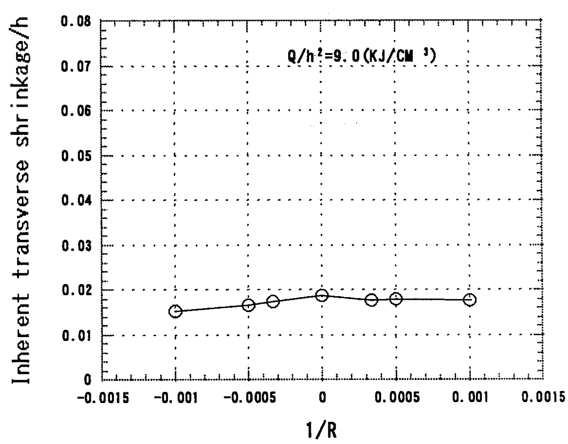

Fig.12 Effect of curvature on inherent shrinkage.

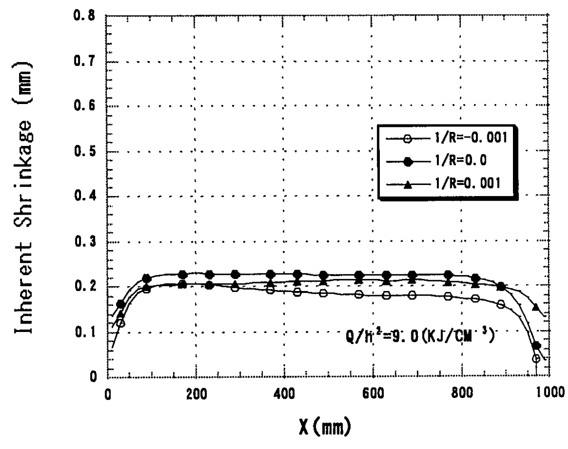

Fig.13 Comparison between distribution of inherent shrinkage in plates with different curvature.

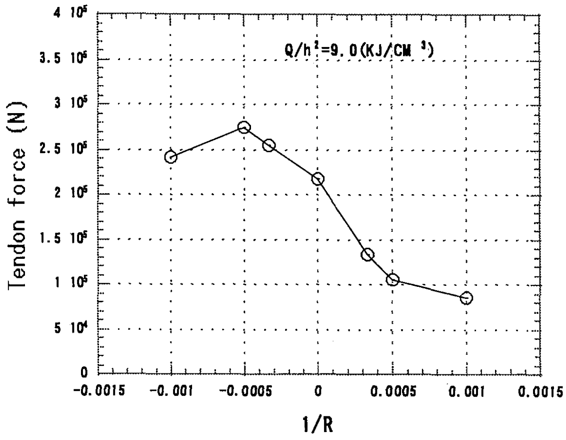

Fig.14 Effect of curvature on Tendon Force.

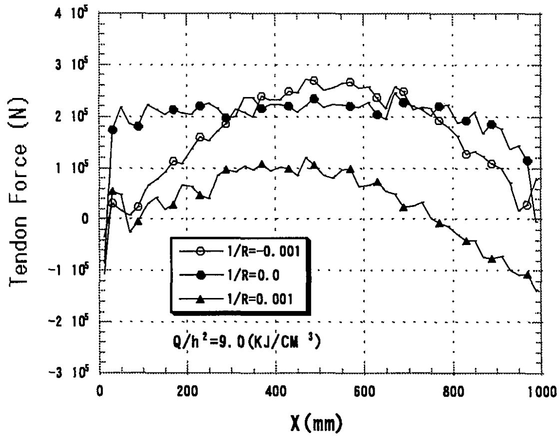

Fig.15 Comparison between distribution of Tendon Force in plates with different curvature.

as an example. The difficulty in the elastic computation is that both the in-plane and the bending inherent strains must be introduced into the elastic FEM model. As one of the easiest ways, a method using a two layer anisotropic plate model is proposed.

4.1 Welding deformation of flat plate

As discussed in section 2, the inherent transverse shrinkage, the inherent angular distortion and the tendon force distribute almost uniformly along the welding line, except near the starting and the finishing ends in the case of bead welding on a flat plate. Thus, it is reasonable to approximate that the inherent deformations and the tendon force distribute uniformly. The possibility of the prediction of welding deformation using this assumption is examined in the following sections.

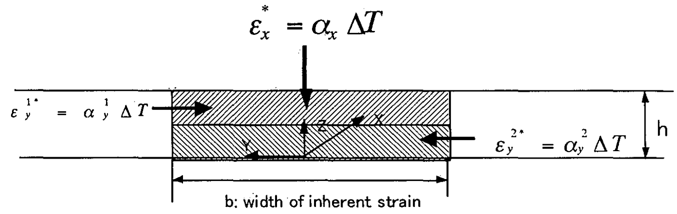

Fig.16 Distribution of inherent strain.

4.1.1 Equivalent strain for two layer plate model

As is readily understood from Eqs. (1), (2) and (3), which define the tendon force and the inherent deformations, the inherent strain distributions which give the same values of the tendon force and the inherent deformation are not unique. Many possibilities exist and these are referred to as equivalent inherent strain distributions. In case of ABAQUS, it is convenient to use the multi-layer anisotropic plate element (S4R) to describe the equivalent inherent strain.

Figure 16 shows the transverse section of the region where the equivalent inherent strain distributes. The X-coordinate and Y-coordinate correspond to the welding direction and the width direction, respectively. The width of the area where the equivalent inherent strain distributes is b. The strain components to be considered are in the transverse and the longitudinal directions. The component of the equivalent inherent strain in the transverse direction ε_y^* forms the transverse shrinkage and the angular distortion. These components are assumed to distribute in two layers with the same thickness. The equivalent inherent strains distribute uniformly in each layer but the values ε_y^{*1} and ε_y^{*2} are different. According to the definition of the equivalent inherent strain, these are given by the following equations.

$$\varepsilon_y^{1*} = (\delta_y - \tfrac{2}{3}h\theta)/b \qquad (7)$$
$$\varepsilon_y^{2*} = (\delta_y + \tfrac{2}{3}h\theta)/b \qquad (8)$$

In the computation using ABAQUS, these inherent strains are given as the thermal strain under the temperature change of ΔT i.e.,

$$\varepsilon_y^{*1} = \alpha_y^{*1}\Delta T \qquad (9)$$
$$\varepsilon_y^{*2} = \alpha_y^{*2}\Delta T \qquad (10)$$

where, α_y^{*1} and α_y^{*2} are the thermal expansion coefficients of each layer. On the other hand, the component of the equivalent inherent strain in the longitudinal direction ε_x^* corresponds to the tendon force F through Eq.(1). Assuming that the equivalent inherent strain component ε_x^* distributes uniformly

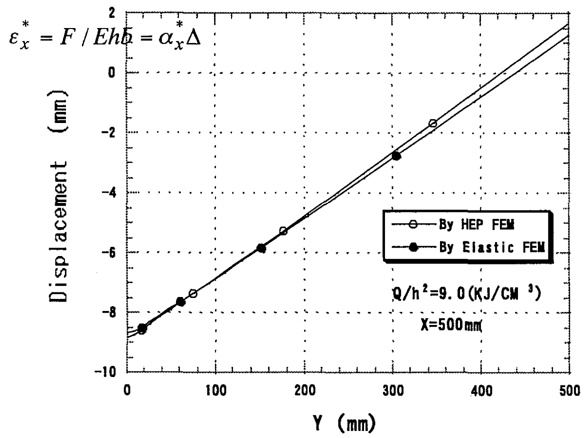

Fig.17 Displacement in Z direction on middle cross-section.

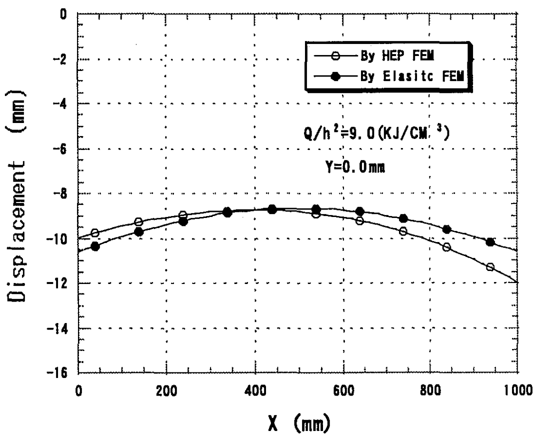

Fig.18 Displacement in Z direction on welding line.

across the thickness, its value can be determined by the following equation.

$$\varepsilon_x^* = F/Ehb = \alpha_x^*\Delta T \qquad (11)$$

4.1.2 Results of elastic computation

The same problems analyzed by thermal-elastic-plastic FEM in section 2 are analyzed by elastic FEM using the equivalent inherent strain. In the elastic analysis, the element S4R in the ABAQUS element library is used. The same in-plane mesh division as in the thermal-elastic-plastic analysis is used.

Taking the case-3 (Q/h^2=9.0 kJ/cm^3) as an example, the deflections computed by the thermal-elastic-plastic analysis and the elastic analysis are compared in **Figs. 17** and **18**. The deflection along the transverse section at the center and that along the welding direction are shown in these figures, respectively. As it is observed from these figures, the welding deformation computed by the thermal-elastic-plastic analysis using the solid elements is accurately reproduced by the elastic analysis using the plate element. Agreements with the same degree are generally observed in other cases. This suggests that the welding deformation can be accurately predicted by the elastic plate analysis if the inherent deformations and the tendon force are known.

4.2 Welding deformation of plate with longitudinal curvature

4.2.1 Assumption on equivalent inherent strain

As discussed in section 3, the following conclusions are drawn from the thermal-elastic-plastic FEM analysis of curved plate.

1) The distribution and the value of the inherent transverse shrinkage for the curved plate and the flat plate are almost the same.
2) The inherent angular distortion in the curved plate distributes almost uniformly except near the starting and the finishing ends as in the case of the flat plate. However, the values of the inherent angular distortion are different between them.
3) The value and the distribution of the tendon force in the curved plate are quite different from those of the flat plate and they vary with the magnitude of the curvature.

Generally, inherent transverse shrinkage is not influenced by the curvature but its influence is large on inherent angular distortion and the tendon force. Considering the practical application, it is relatively easy to compute or to measure the inherent deformation and the tendon force of a welded flat plate. But, it requires great effort to obtain these values for plates with arbitrary curvatures. Thus, if the inherent deformations and the tendon force for the flat plate can be used to predict the welding deformation of the curved plate, the procedure of predicting the welding deformation of structures with arbitrary form can be greatly simplified. To clarify the possibility of such a simplified method, the welding deformations of the curved plates are computed by the elastic FEM using the inherent deformations and the tendon force of the flat plate.

4.2.2 Results of elastic computation

The procedure of the computation is basically the same as in the case of the flat plate. Only the z-coordinate of the plate is changed according to Eq. (6). The case-3 with (Q/h^2=9.0 kJ/cm^3) is selected as an example. The welding deformations of plates with six different curvatures are computed using the equivalent inherent strain defined for the two layer plate model as discussed in section 4.1.1.

The deflection along the transverse section at the center and that along the welding direction are shown in **Figs. 19** and **20**. The deflections directly computed by the 3-dimensional thermal-elastic-plastic FEM analysis are compared with those predicted by elastic FEM using the inherent deformations and the tendon force. The plate with longitudinal curvature of 1/R=0.005 is taken as an example. As it is seen from Fig.19, the deflection on the transverse section can be accurately predicted by the elastic analysis. Relatively large errors are observed in the deflection along the welding direction, as is shown in Fig. 20.

The transverse bending and the longitudinal bending are compared between the thermal-elastic-plastic analysis and the elastic analysis of plates with different values of curvature in **Figs. 21** and **22.** The transverse bending and the longitudinal bending are the deflection at the center of the plate relative to the line connecting two edge points on the transverse and the longitudinal sections, respectively. The transverse bending decreases with the magnitude of the curvature of plate. The error in the prediction by the elastic analysis is very small. On the other hand, the error in the longitudinal bending is relatively large. This error comes from neglecting the difference of the tendon force between the curved plate and the flat plate which is shown in Fig. 15. However, the absolute value of the error in the longitudinal bending is less than 2 mm. If an error of this magnitude can be allowed, the welding deformation of the curved plate can be predicted by the elastic plate analysis using the inherent deformation and the tendon force.

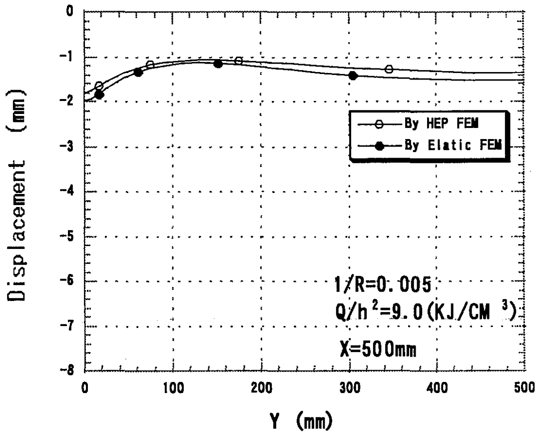

Fig.19 Displacement in Z direction on middle cross-section.

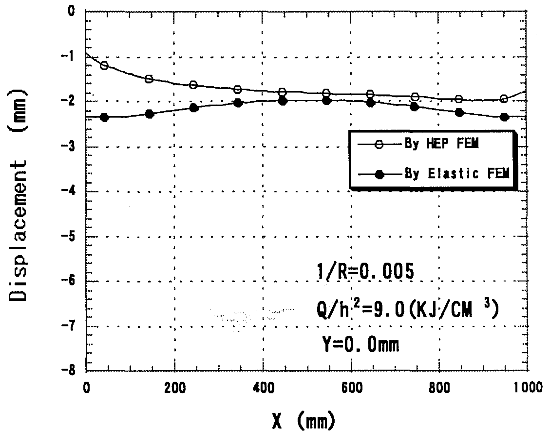

Fig.20 Displacement in Z direction on welding line.

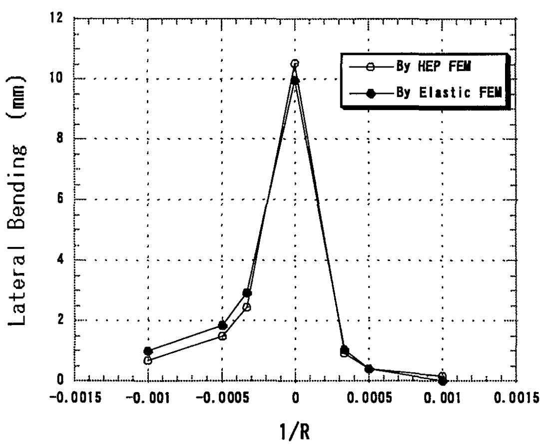

Fig.21 Effect of curvature on lateral bending.

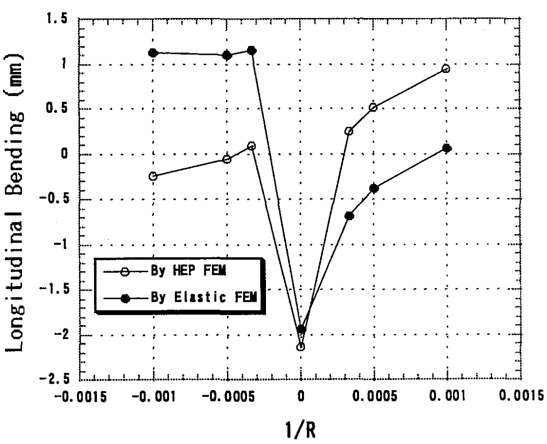

Fig.22 Effect of curvature on longitudinal bending.

5. Conclusions

Welding deformation of plates with longitudinal curvature has been analyzed by thermal-elastic-plastic FEM. The phenomena are clarified from the aspect of the inherent strain and the following conclusions are drawn.

1) The inherent deformations and the tendon force are directly computed as integrations of plastic strain obtained by the thermal-elastic-plastic FEM analysis. Based on the computed results, the effect of heat input and the distribution of the inherent deformations and the tendon force are closely examined for both flat plate and plate with longitudinal curvature.
2) A method using a two layer anisotropic plate element in ABACUS and the equivalent inherent deformations and the tendon force is proposed to predict the welding deformation by elastic analysis. Its validity is examined through comparisons with the welding deformations directly computed by the thermal-elastic-plastic FEM.
3) It is shown that the welding deformation of plates with longitudinal curvature can be accurately predicted by the elastic plate analysis using the inherent deformations and the tendon force for the flat plate.

References

1) Y. Ueda and N. X. Ma, "Expression of Inherent strain in Form of Function and its Estimation, -Estimating and Measuring Methods of Residual Stresses Using Inherent Strain Distribution Described as Functions (Report 1) ", Trans. Japan Welding Soc., Vol1 (1993), No.1,189-195(in Japanese).
2) H. Murakawa, Y. Luo, Y. Ueda, "Prediction of Welding Deformation and Residual Stress by Elastic FEM Based on Inherent Strain (First Report) -Mechanism of Inherent Strain Production", *Trans. Soc. Naval Architects of Japan*, 1996, **180**, 739-751(in Japanese).
3) Y. Luo, H. Murakawa, Y. Ueda, "Prediction of Welding Deformation and Residual Stress by Elastic FEM Based on Inherent Strain - (Third Report) Deformation and Residual Stress in Narrow Gap Welding ", *Trans. Soc. Naval Architects of Japan,* 1997,**182**(in Japanese).